a-Si:H electron drift mobility measured under extremely high electric field

J. Kočka, O. Klíma, and E. Šipek
Institute of Physics, Czech Academy of Sciences, Cukrovarnická 10, 162 00 Praha 6, Czechoslovakia

C. E. Nebel and G. H. Bauer
Institute für Physikalische Elektronik, Universität Stuttgart, Pfaffenwaldring 47, W-7000 Stuttgart 80, Federal Republic of Germany

G. Juška
University of Vilnius, Saueletkio aleja 9, 3K., 232 054 Vilnius, Lithuania

M. Hoheisel
Siemens A. G. Corporate Research and Development, Otto-Hahn-Ring 6, W-8000 München 83, Federal Republic of Germany
(Received 9 April 1991; revised manuscript received 7 October 1991)

The electron drift mobility of undoped *a*-Si:H is studied by a current time-of-flight method over a broad temperature range ($T=35-300$ K). A possibility of deducing the drift mobility (μ_D) from the initial ($t=0$) value of space-charge-limited current (SCLC) is suggested and verified for $T>120$ K. In the SCLC case an effect, the so-called pseudotransit, is observed and explained. The drift mobility is deduced at electric fields $F>1\times10^5$ V/cm and low temperatures, $T<120$ K, not only for a high intensity of illumination (the SCLC case) but also for the "small-signal" case (low-intensity illumination). Both these values are in agreement, and there is no increase of μ_D at $T<100$ K, as observed by W. E. Spear [in *Amorphous Silicon and Related Materials,* Advances in Disordered Semiconductors Vol. 1, edited by H. Fritzsche (World Scientific, Singapore, 1989), p. 721]. The strong electric-field dependence of the collected charge is observed at these temperatures and even at 40 K almost full charge collection is reached. This implies that the quantum efficiency $\eta\approx1$. In the end, two possibilities of explaining the discrepancy in comparison with Spear's work are discussed.

I. INTRODUCTION

It is of great importance to understand the transport and recombination of nonequilibrium carriers in amorphous hydrogenated silicon (*a*-Si:H). Recently, following the pioneering papers by Spear,[1] the low-temperature (T) region has generated some interest. Below $T\approx100$ K a predominantly hopping transport has been discovered[1] by use of a time-of-flight (TOF) technique, with the drift mobility (μ_D) being surprisingly high and a function of light intensity.

Independently the traveling-wave technique[2] has been used for the study of μ_D of *a*-Si:H. The existence of the low-T hopping regime has been confirmed, but much lower drift mobilities, independent of light intensity, have been found.[2] However, recently the discovered[3] technical problems of the traveling-wave technique have questioned the possibility of using it below 100 K.

With decreasing temperature the current, detected by the TOF method, decreases and detection becomes difficult. One of the solutions to the problem of how to increase the sensitivity is to use the so-called integral mode[1] TOF. However, a recent TOF study[4] in the subnanosecond time region has shown that in the integral mode TOF (Ref. 1) under the space-charge-limited current (SCLC) conditions, the apparent[4] increase of μ_D (related to the screening current—see below) can be deduced when the absorption depth of the light is a nonnegligible part of the sample thickness (d). Due to the general decrease of the drift mobility with decreasing temperature, the effect of screening may play a serious role. In this paper we use the current-mode TOF and our aim is to compare the results deduced in both the SCLC and the "small-signal" case. In the small-signal case the charge created by light (Q_0) is smaller than the charge on the electrodes (equal to CU_0, where C is the sample capacity and U_0 the applied voltage).

II. EXPERIMENTAL DETAILS

For the TOF measurement we used high-quality *a*-Si:H *p-i-n* junctions with the thickness $d=5.7$ and 10 μm. High quality, necessary to withstand the high electric field, mainly means extremely low reverse dark current. For this purpose special precautions (such as etching of the n^+ layer outside the metal contacts) are necessary.

For the TOF measurement we have used three apparatuses. In Prague and Stuttgart, standard arrangements were used with Iwatsu TS-8123 and Hewlett-Packard 54111D oscilloscopes for time $t\geq10$ ns.

The *p-i-n* junction was illuminated through the *p* side by a 3-ns-long laser pulse, generated by a Laser Science nitrogen-pumped dye laser (typically with $\lambda=530$ nm). When the averaging was used the repetition rate of laser pulses was typically 0.1 Hz.

An optical fiber was used between the laser and the sample holder. The resulting time delay eliminates the electromagnetic noise related with the laser pulse. The

full power (100%) of the laser (behind the fiber) created in *a*-Si:H typically the charge $Q_0 = 1 \times 10^{-8}$ C. This can fluctuate slightly from sample to sample as a function of the contact transparency. The sample holder allows us to control the temperature in the range 30–300 K.

The voltage pulse (up to 500 V) was applied to the *p-i-n* junction typically 10–100 μs before the laser pulse. This delay is long enough to guarantee voltage stabilization but short enough to prevent field redistribution inside the *p-i-n* junction. Due to the selected voltage polarity (the illuminated *p* side being negative) the blocking nature of the contacts was guaranteed and the experimental current transients were dominated by the transport of electrons.

For the current detection we used resistors with $R = 50$–$200\ \Omega$ (as a standard, a 50-Ω resistor was used; resistors with higher resistivity were used for increasing sensitivity at longer times). In this case the RC constant was $RC \ll t_T$ (where t_T is the small-signal transit time), which is a typical indication of the current-mode TOF. This is the basic difference in comparison with Ref. 1 in which the integral mode TOF (R of the order of $M\Omega$) was used.

The third setup used at Vilnius University is able to measure with the subnanosecond time resolution. Its details are described elsewhere[5] because we have used only a few points gained on this setup (see Fig. 3).

III. EXPERIMENTAL RESULTS

The typical current transients measured at different temperatures at 50 V on a 10-μm *p-i-n* junction in the small-signal case are shown in Fig. 1. With decreasing temperature the nondispersive character of the current transients (flat current before the carrier extraction) changes to the dispersive one, and the overall current decreases.

Following the results of Spear,[1] the drift mobility below $T \approx 100$ K should increase again and so, in our first measurement at $T = 40$ K, we concentrated on the time region ($t \approx 10^{-7}$ s) corresponding to the expected transit time.[1] The first results measured on a 5.7-μm *p-i-n* junction in the small-signal case are depicted in Fig. 2. To be able to measure we had to increase the voltage to 120 V (electric field $F = 2.1 \times 10^5$ V/cm). However, no sign of

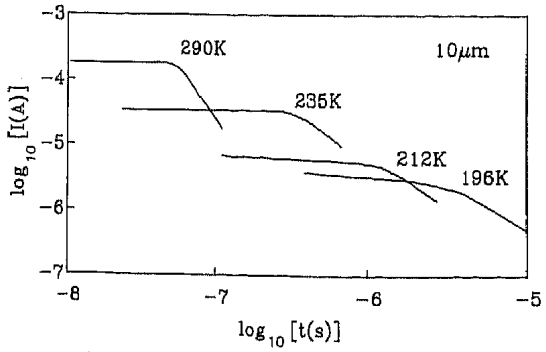

FIG. 1. The current transients measured under the "small-signal" conditions on a 10-μm-thick *a*-Si:H *p-i-n* junction at 50 V and different temperatures.

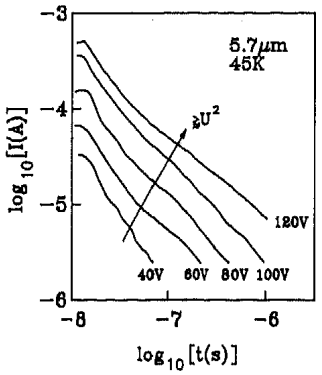

FIG. 2. The current transients measured under the small-signal conditions on a 5.7-μm-thick *a*-Si:H *p-i-n* junction at 45 K and different voltages.

the typical current transient, corresponding to the transit of carriers, has been observed.

Moreover, with increasing voltage the current increased more than quadratically. One reason could be that the drift mobility increases with the voltage; the second possibility is the influence of the space-charge effects. The accumulation of charge from the previous pulses can also play a role at very low temperatures.

These reasons stimulated us to change the philosophy and to intentionally use the SCLC conditions (high-laser intensity). The first advantage in this case is that the signal is higher (easier detection) and secondly the influence of the remaining charge from the previous pulses is less important.

A standard way of deducing the drift mobility in the SCLC mode is to deduce the time, corresponding to the so-called "cusp" (maximum) position which is equal to 0.78 of t_T (transit time).[6] The typical room-temperature signal in SCLC mode is displayed in the inset of Fig. 3; the vertical arrow indicates the cusp position.

However, with decreasing temperature and/or increasing trapping,[6] the cusp is more and more smeared and difficult to identify. However, there is one point[6] which in any case could be used to find the drift mobility. This is the initial ($t = 0$) value of the SCL-current which, fol-

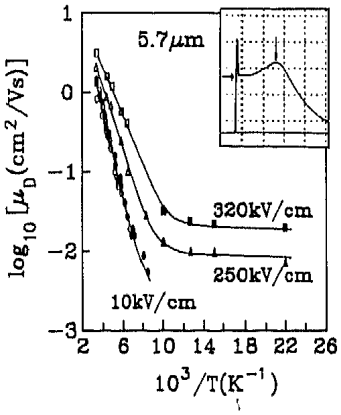

FIG. 3. The electron drift mobility (μ_D) as a function of temperature (T) for different electric fields (F): full points are deduced from the initial SCL-current value (see inset and text), ○ from the "cusp" position, and △ and □ from the subnanosecond "small-signal" TOF measurements (Ref. 5). See text for explanation of inset.

lowing Ref. 6, is given by

$$I_{\mathrm{SCLC}}(t=0)=\frac{1}{2}\frac{CU_0}{t_T}=\frac{\epsilon_0\epsilon S}{2d^3}U_0^2\mu_D\ , \tag{1}$$

where ϵ_0 and ϵ are absolute and relative permittivities and S is the area of current region [in Ref. 7 the factor $\frac{9}{8}$ has been erroneously included]. The initial SCL-current value (see left arrow in the inset of Fig. 3) represents a simple method of finding μ_D. The initial spike (usually associated with the built-in field, back diffusion but in the SCLC case mainly with the screening current[5]) can be, on the linear scale, eliminated with reasonable accuracy. In practice we have defined the initial I_{SCLC} as a current at $t=10$ ns. The proof of the accuracy of this interpretation is the independence from light intensity.

When we deduced the drift mobility at room temperature (RT) from the signal, displayed in the inset of Fig. 3 in both ways (cusp position and the initial I_{SCLC} value) the agreement was very good. To test this idea more carefully we studied the temperature dependence of the electron drift mobility by both methods. From Fig. 3 it can be seen that the agreement is very good again and that the initial I_{SCLC} method can be used to lower temperatures.

Below 100 K and at $F<10^4$ V/cm, even the SCLC transient is difficult to detect. From Fig. 4 it is seen that although the initial part of the signal for 100 V ($F=1.75\times10^5$ V/cm) is easily detected, it is rather featureless. For $F>2\times10^5$ V/cm, the shape of the current transients dramatically changes.

The full circles on the vertical axis in Fig. 4 represent the initial I_{SCLC} from which the drift mobility at 45 K has been calculated and plotted in Fig. 3. For the study of the temperature dependence of the drift mobility at high electric field ($F>2\times10^5$ V/cm) and low temperatures, the initial I_{SCLC} value has been used. For high temperatures ($T>130$ K), see Fig. 3, these results have been combined with the small-signal results, measured on an *identical sample* with the subnanosecond setup. The important conclusion drawn from the first results, displayed in Fig. 3, is that at low temperatures the temperature dependence of the drift mobility is rather flat and no increase[1] is observed.

There is a question of the significance of the strongly

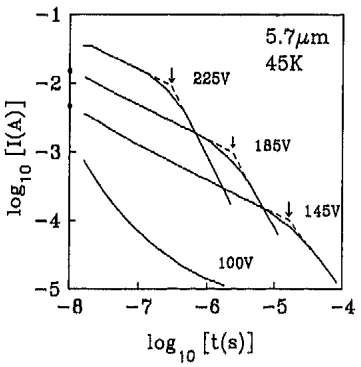

FIG. 4. The current transients measured at full laser intensity (100% L) on a 5.7-μm-thick a-Si:H p-i-n junction at 45 K and different voltages. The full points on the current axis are the values taken as initial I_{SCLC}.

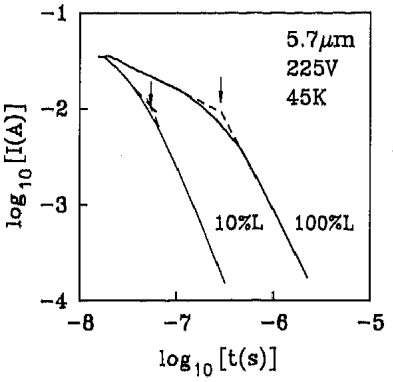

FIG. 5. The current transients measured at full laser intensity (100% L) and 10 times reduced intensity (10% L) on a 5.7-μm-thick a-Si:H p-i-n junction at 45 K and 225 V.

voltage-dependent transients displayed in Fig. 4. We call such a transient "pseudotransit" and its origin is related to the "extraction time" qualitatively explained in Fig. 5. For 10% laser intensity (L) the charge created by light (Q_0) is in the vicinity of SCLC regime ($Q_0<CU_0$). The change in the slope of the current transient at about 50 ns is of the order of true transit time. When we increase the laser intensity (see the 100% laser intensity curve in Fig. 5) the charge $Q_0\gg CU_0$; however, the maximum charge which can be transported through the sample is still CU_0. The remaining charge waits in the region of generation. Due to the fact that we are in the current-mode TOF when the charge extraction begins, the external circuit continuously recharges the sample and more and more carriers can be transported until the full charge Q_0 is extracted (or its substantial part). This can lead to a change of the slope of the current transient.

The possibilities and limitations of such a simplified explanation of the extraction time are explained in detail elsewhere.[8] Naturally, the extraction time is a function[8] of the true transit time and this explains the voltage dependence shown in Fig. 4. A similar effect has also been observed for a 10-μm sample for full laser intensity (see Fig. 6). With the decreasing laser intensity the crossover of the current transient becomes independent of laser intensity and represents the true transit time. The fact that the drift mobility, deduced from the small-signal transit time, corresponds to the μ_D value, deduced from the initial I_{SCLC} value, is encouraging. The small-signal transit time of the 10-μm sample is about 10 times longer

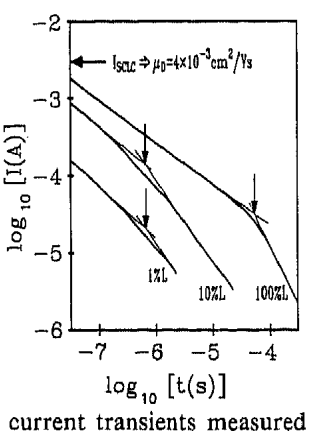

FIG. 6. The current transients measured on a 10-μm-thick a-Si:H p-i-n junction at 45 K and 350 V at different laser pulse intensities (1%, 10%, and 100% L).

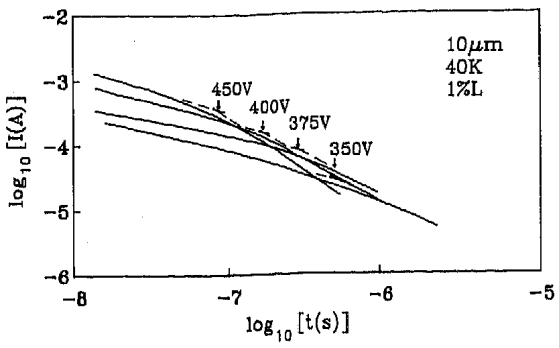

FIG. 7. The current transients measured under the small-signal conditions (1% laser intensity) on a 10-μm-thick *a*-Si:H *p-i-n* junction at 40 K and different voltages. The arrows indicate the "crossover" time.

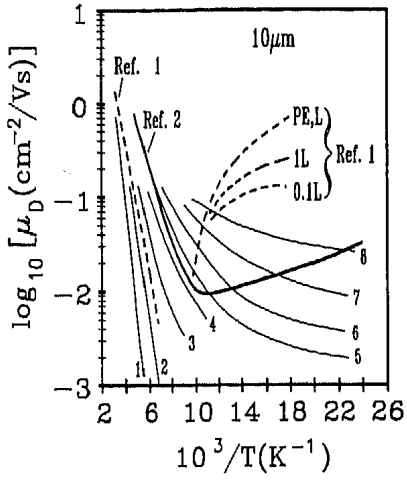

FIG. 9. The small-signal (1% laser intensity) electron drift mobility (μ_D) as a function of temperature for different electric fields. The electric field (in V/cm) for curves 1–8 was as follows: (1) $F=5\times10^4$, (2) $F=2\times10^5$, (3) $F=3\times10^5$, (4) $F=3.5\times10^5$, (5) $F=3.75\times10^5$, (6) $F=4\times10^5$, (7) $F=4.25\times10^5$, (8) $F=4.5\times10^5$. For comparison the results of Ref. 1 (dashed lines) and Ref. 2 (bold line) are shown. [PE denotes the preillumination (Ref. 1), *L* the laser intensity.]

(see Fig. 6) than the 5.7-μm sample (see Fig. 5) due to the existence of the dispersion and the slightly lower electric field used for the 10-μm sample (3.5×10^5 V/cm instead of about 4×10^5 V/cm) which is, however, due to the strong electric-field dependence of μ_D very substantial (see Fig. 11). We have succeeded in detecting the small-signal (1% *L*) transients at low temperatures for the 10-μm sample, however, only at extremely high electric field ($F>3\times10^5$ V/cm). The typical curves measured at different voltages are displayed in Fig. 7.

The drift-mobility value depends on the transit-time definition.[9,10] For nondispersive transport, the time at which the current drops to 50% of its (constant) pretransit value is generally used. For dispersive transport, the crossover point is very often used for the t_T definition (see Fig. 7). Due to the fact that with the decreasing temperature the transport changes from a nondispersive to a dispersive one, it seems to us most suitable to use the so-called "combined-pulse" technique[9] (illustrated for medium temperature in Fig. 8), where the time at which the current drops to 50% of the extrapolated "cover curve" is taken as the transit time. The measured transients are vertically shifted and normalized to the common cover curve. This way basically corresponds to the time-dependent drift-mobility [$\mu^*(t)$] definition.[11]

At room temperature the μ_D values deduced from the different t_T definitions are very close. With decreasing temperature (and increasing dispersion) the difference increases, as seen in Fig. 8. The combined-pulse technique gives the longest t_T, i.e., the lowest μ_D.

Figure 9 shows the temperature dependence of the drift mobility (measured under the small-signal conditions) for different electric fields. These results of ours are compared with the results of Refs. 1 and 2. Not only in the SCLC regime (see Fig. 3), but also in the small-signal case, we have found no sign of increase of the drift mobility as in Ref. 1 (dashed curves). Most evident is the strong electric-field dependence of μ_D for $F>2\times10^5$ V/cm,

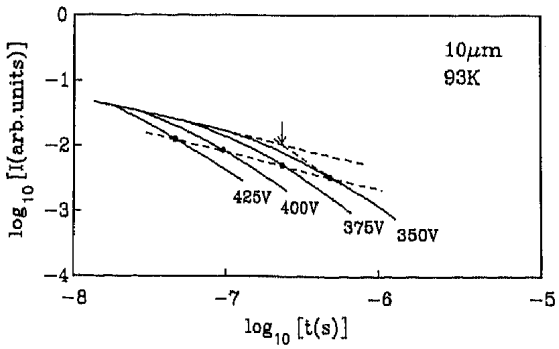

FIG. 8. The current transients measured under the "small-signal" conditions (1% laser intensity) on a 10-μm-thick *a*-Si:H *p-i-n* junction at a medium temperature (93 K) and different voltages. The full circles are the transit times (t_T) deduced by a combined pulse technique (see text); the arrow indicates the crossover definition of t_T (see text) for a 350-V curve.

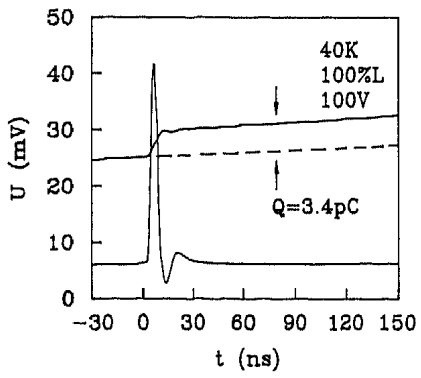

FIG. 10. The current transient (displayed as the voltage measured on a 50-Ω resistor) measured at full laser intensity (100% *L*) on a 10-μm-thick *a*-Si:H *p-i-n* junction at 40 K and 100 V. The integrated charge, recorded at the same time resolution, is also shown. The collected charge $Q=3.4$ pC.

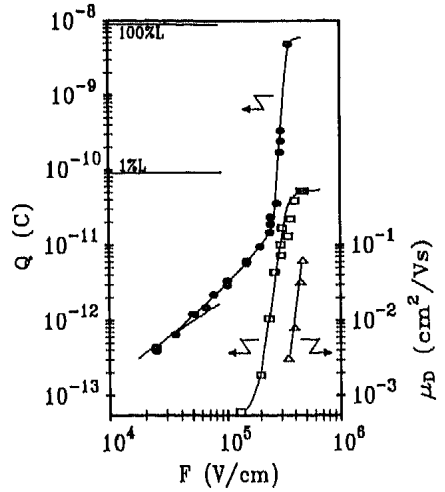

FIG. 11. Collected charge (Q) at $T=40$ K on a 10-μm-thick a-Si:H p-i-n junction as a function of electric field F for 1% (□) and full (100%) laser (●) intensities. Field dependence of μ_D is shown for comparison (△).

which can explain the steady-state photocurrent measurement by Stachowitz, Fuhs, and Jahn.[12]

The value of the drift mobility and its temperature and electric-field dependencies are very important. However, equally important information can be gained from the so-called charge-collection dependence. Figure 10 depicts one transient and also integrated charge, measured in parallel at 40 K, with the full laser intensity and at *relatively* low electric field ($F=1\times10^5$ V/cm). Figure 11 shows the whole charge-collection curve (i.e., the collected charge as a function of the applied electric field) for two laser intensities (1% and 100%).

From Fig. 11, and also from Fig. 10, it is seen that at 40 K for $F<1.5\times10^5$ V/cm the collected charge is less than 1% of the charge generated by light. Moreover, a substantial part of the collected charge at these fields is related to the initial spike (see Fig. 10). The charge integration time in Fig. 10 is about 100 ns. Although prolonging the integration time would partially increase the collected charge, it is clear that at these fields ($F<1.5\times10^5$ V/cm) the trapping is so strong that it is almost impossible to observe the charge transit.

On the other hand, with increasing electric field (see Fig. 11) the collected charge strongly increases, saturates, and approaches the charge created by light. Such an almost-full collection is strong support for our statement that for $F>3\times10^5$ V/cm we observe the real transit of carriers.

The collected charge Q is proportional to the product of $\eta\mu_D\tau_D$, where η is the quantum efficiency of free-charge generation and $(\mu_D\tau_D)$ the product of the drift mobility and deep trapping time. Generally all three quantities can be field dependent. The fact that the increase of the collected charge ($\approx\eta\mu_D\tau_D$) is almost parallel to the field dependence of the drift mobility (see Fig. 11) tells us that the electric-field dependence of η is rather weak (if any). The drift-mobility values in Fig. 11 are deduced from the crossover points in Fig. 7 and so μ_D is higher than the values in Fig. 9 deduced by a combined-pulse technique. We estimate from Fig. 11 that the η is almost 1 at this electric field.

IV. DISCUSSION AND CONCLUSIONS

The drift mobility of a-Si:H, sharply increasing[1] below 100 K, was rather an unexpected result, which stimulated a few groups to continue the study of low-T transport. Preliminary results gained by a different technique, the traveling-wave technique,[2] confirmed the increase of the drift mobility below 100 K. However, a recent paper[3] questioned the validity of traveling-wave results below 100 K.

Our first results,[7] gained from the SCLC transients, indicated that there is no increase of μ_D below 100 K. The fact that the mobility values deduced from the small-signal TOF agree very well with our SCLC data, and that we have reached nearly full charge collection, represent strong proof that we are observing the real transit of charge and that our μ_D values are correct.

Our results are supported by a recent study[13] of dc conductivity of doped a-Si:H samples down to the He temperatures. The drift mobilities deduced from these measurements continuously decrease (as well as our data) with the decreasing T and no increase of μ_D below 100 K is observed.

There is one important question of how to explain the difference between the results of Spear[1] and our results, which are clearly demonstrated in Fig. 9. There are basically two possible explanations.

The first possibility is that our samples and samples used in Ref. 1 are very different. The recent model calculations by Kemp and Silver[14] have shown that the low-temperature drift mobility may be a very sensitive function of the shape of the tail states, and a sharp drop of density of states can lead to the increase of μ_D at low T as illustrated in Fig. 12. If this is the cause, we have a very

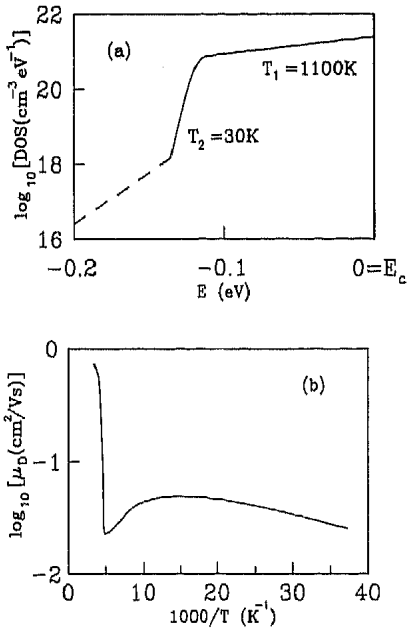

FIG. 12. The model density of states (a) where the full line corresponds to the density of states given by Eq. 10 of Ref. 14, with the sharp exponential drop in the tail-state density (described by the characteristic temperature $T_2=30$ K) and the resulting calculated temperature dependence of the drift mobility (b) taken from Ref. 14.

sensitive tool for the study of tail-state density. The second possibility is that the interpretation of the experimental results of Spear[1] (about which we have no doubts) has to be modified.

There are indications[15] that at $T < 100$ K there is $\eta \approx 1$ not only at extremely high electric fields (see Fig. 11) but also in the whole range 10^4 V/cm $< F < 10^5$ V/cm used in Ref. 1. If $\eta \approx 1$ instead of $\eta \approx 0.05$, as claimed in Ref. 1, then the real photogenerated charge Q_0 was[1] probably much higher, $Q_0 > CU_0$, and the SCLC effects could play an important role.

In Ref. 1, the integral-mode TOF has been used; to facilitate comparison we also assume the integral-mode TOF for further discussion. The integral-mode SCLC transient has two parts[15,16]—the screening current in the photogeneration region and the drift to the unilluminated electrode (see the Appendix and Fig. 13).

When the drift mobility is small and the electric field is also small, the charge induced on the electrodes by the drift of the carriers is small and persists for a much longer time than the screening current and in the short-time region the screening current is dominant.

The voltage transient associated with the screening current[16] (see the Appendix) is similar to the small-signal drift and the "screening time" t_s is given by the equation

$$t_s = \Delta U \left[\frac{dU}{dt} \right]^{-1} \Bigg|_{t=0} , \tag{2}$$

where for $Q_0 > CU_0$ the ΔU (magnitude of the voltage step in integral-mode TOF used in Ref. 1) is given (see Fig. 13) by[16]

$$\Delta U = U_0 \frac{1 + \ln(Q_0/CU_0)}{\alpha d} , \tag{3}$$

where α is the absorption coefficient for a given laser wavelength. The screening-induced ΔU step, superimposed on the standard SCLC signal, is illustrated in Fig.

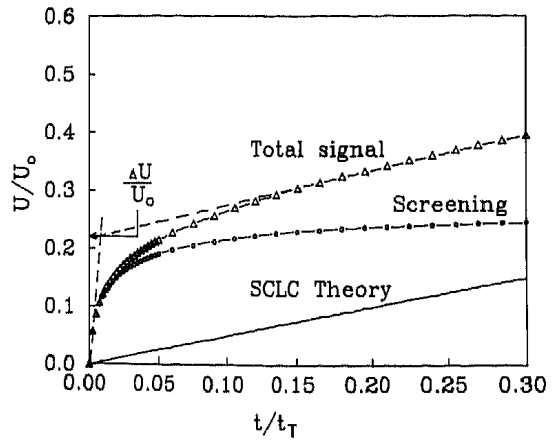

FIG. 13. The computed time dependence of the voltage transient U/U_0 in the integral-mode TOF for the case of standard SCLS theory (full line) and for the case with included screening contribution (see the Appendix) (curve labeled "total signal," Δ). The screening contribution itself is displayed as well ($\circ$). U_0 is the applied voltage and t_T the small signal transit time. For the calculation of screening and total signal curves the parameters $L' = 30$ and $\alpha' = \alpha d = 20$ have been used (see text).

13. The initial voltage transient slope is[16]

$$\left. \frac{dU}{dt} \right|_{t=0} = \frac{Q_0}{Ct_T} , \tag{4}$$

where t_T is the real transit time.

This equation rewritten in normalized units, used in Fig. 13, is

$$\left. \frac{d(U/U_0)}{d(t/t_T)} \right|_{t=0} = \frac{Q_0}{CU_0} = L' , \tag{5}$$

from which it is clear that the initial slope is proportional to the normalized laser intensity (L').

If we take t_s as an apparent transit time, we will get, for the apparent mobility μ_s the expression

$$\mu_s = \mu_D(U_0) \frac{Q_0}{CU_0} \frac{\alpha d}{1 + \ln(Q_0/CU_0)} , \tag{6}$$

where we assume that, in general, the true drift mobility can be a function of U_0.

Because for strongly absorbed light (used in TOF) $\alpha d \gg 1$, the ratio $\Delta U/U_0 \ll 1$ and the screening transient looks like the small-signal case. Following Eq. (6) we can get the apparent mobility $\mu_s \gg \mu_D$, which is a sublinear function of light intensity (Q_0), as observed in Ref. 1.

In Ref. 1 it was found that the measured mobility (which we believe is μ_s) is independent of U_0. To explain this fact $\mu_D(U_0)$ should be a sublinear function of U_0 [see Eq. (6)]. The results presented in Fig. 11 (the superlinear

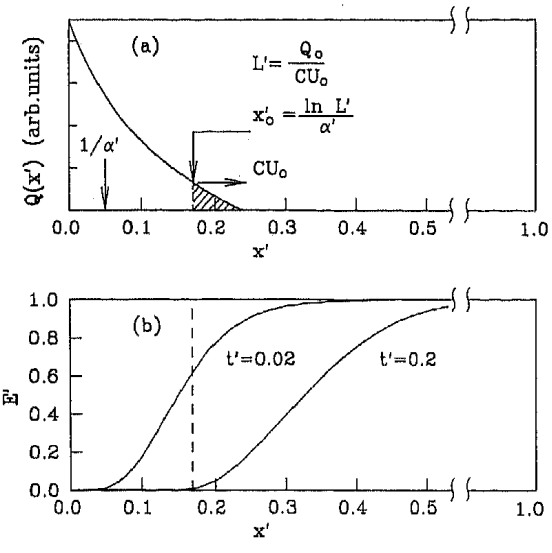

FIG. 14. (a) The schematic illustration of the charge-profile $Q(x')$ generated by a laser pulse, "normalized absorption depth" $1/\alpha'$, where $\alpha' = \alpha d$ (α is the absorption coefficient, d the sample thickness) and the starting position (x'_0) of the first CU_0 charge. The coordinate x' is the position normalized to the sample thickness $x' = x/d$. Parameters used for calculation are $\alpha' = \alpha d = 20$, $L' = 30$. (b) The space profile of the electric field (E') at two times (t'). All quantities are given in dimensionless ("normalized") units. $E' = E/E_0$, where $E_0 = U_0/d$; $x' = x/d$; $t' = t/t_T$, and t_T is the small-signal transit time. The dashed line corresponds to x'_0 from part (a). Parameters used for calculations are $\alpha' = \alpha d = 20$, $L' = 30$.

increase of the collected charge in the range of electric fields 10^4 V/cm $< F < 10^5$ V/cm together with the low-T photoconductivity data[12] and recent results of Antoniadis and Schiff[17] indicated such a situation.

In a recent paper[15] we have used the parameters employed in Ref. 1 and, utilizing Eq. (6), we have numerically modeled the voltage dependence of $1/t_s$ for different laser intensities. These simulations fit well to the original experimental data for Ref. 1.

We want to remark that, following the above interpretation of the screening current, for the opposite electric field, suitable for the study of the drift of holes, a similar qualitative signal has to be observed even if only electrons could move.

To conclude this discussion we wish to say that the study of low-T transport, especially for high electric fields, is rather a difficult job. That is why only a limited number of papers[17–19] have recently appeared, and clearly more information is necessary before the definitive conclusions can be drawn.

At present we can draw the following tentative conclusions.

(1) We have suggested and verified a way of deducing the value of the drift mobility, based on the initial value of the space-charge-limited current (I_{SCLC}).

(2) Using extremely high electric fields (up to 4.5×10^5 V/cm) we have succeeded in deducing the electron-drift mobility in a-Si:H at $T < 120$ K under the SCLC conditions but also in the small signal case. Both values are in reasonable agreement.

(3) The observed drift mobility (μ_D) is independent of light intensity and continuously decreases with decreasing temperature. No increase of μ_D at $T < 120$ K has been observed.

(4) The drift mobility at $T < 120$ K is strongly field dependent.

(5) We believe that the proportionality of the transit time to $(1/U_0)$ is not sufficient proof of the real transit. The collection of a substantial portion of light-generated carriers is a necessary condition.

(6) At high electric field ($F > 3\times10^5$ V/cm) even at 40 K, nearly full charge collection is observed, which supports our statement that we are observing the real transit of carriers. The strong increase of collected charge is given mainly by the strong increase of $\mu_D(F)$. At these electric fields the quantum efficiency approaches 1 (about 0.7) and is only slightly (if at all) field dependent.

(7) We have observed, under SCLC conditions, the so-called pseudotransit and qualitatively explained it as an extraction time.

(8) We have discussed two possible explanations for the difference between our results and the results in Ref. 1. We believe that the combined effects of the field-dependent μ_D and screening current explains the apparent increase of the μ_D below $T = 100$ K.

ACKNOWLEDGMENTS

This work and the stay of one of us (J.K.) at Stuttgart University has been supported by BMFT Contract No. 0328327D. The contribution of Y. Xiao at the initial stage of this work is acknowledged.

APPENDIX

In the standard TOF it is usually assumed that the charge, generated by a laser pulse, is generated by an ideal source, i.e., in an infinitely thin surface layer within an infinitely short time. However, when the charge, generated by a laser pulse (Q_0), is higher than the charge on the electrodes equal to CU_0 (where C is the sample capacity and U_0 the applied voltage), it has been shown[4,8] that the screening current in the generation region and the realistic absorption profile play an important role.

Let us assume that we have a sample (see Fig. 14) with the thickness d and a semitransparent contact through which the sample is illuminated. By the laser pulse we instantaneously generate a charge profile, given by the realistic absorption law (see Fig. 14). We further assume that the so-called integral-mode TOF is used ($RC \gg t_T$, where R is the resistance of the detection resistor and t_T is the small-signal transit time) and at time $t = 0$ the electric field (E_0) is homogeneous and equal to $E_0 = U_0/d$.

To simplify the situation we assume that only one type of carrier (say, positive for mathematical simplicity—it means holes) is mobile. Immediately after the photogeneration the movement of all mobile carriers (holes) leads to the field redistribution.

The kinetics of the field redistribution (when the recombination is neglected) is given by the Poisson and current flow equations

$$\frac{\partial E'(x',t')}{\partial x'} = p'(x',t') - n'(x',t') , \tag{A1}$$

$$\frac{\partial E'(x',t')}{\partial t'} + E'(x',t')p(x',t') = 0 , \tag{A2}$$

$$\frac{\partial n'(x',t')}{\partial t'} = 0 , \tag{A3}$$

where we have introduced "normalized" (dashed) units as follows. The concentration of electrons (n) and holes (p) are given in the units of charge on the electrodes

$$n' = \frac{ned^2}{\epsilon\epsilon_0 U_0}, \quad p' = \frac{ped^2}{\epsilon\epsilon_0 U_0} , \tag{A4}$$

where S is the sample area and ϵ and ϵ_0 are the relative and absolute permittivities. $E'(x',t')$ is the electric field given in the units of the initial field $E'(x',t') = E(x',t')(d/U_0)$, x' and t' are the position and time, respectively, given in units $x' = x/d$ and $t' = t/t_T$.

As boundary conditions ($t = t' = 0$) we assume $E'(x',0) = 1$, $p'(x',0) = n'(x',0) = L'\alpha' \exp(-\alpha' x')$, where L' is the laser-generated charge Q_0, normalized to the charge on the electrodes (CU_0),

$$L' = \frac{Q_0}{CU_0} = \frac{Q_0 d}{\epsilon\epsilon_0 S U_0} \tag{A5}$$

and $\alpha' = \alpha d$, where α is the absorption coefficient.

The combination of Eqs. (A1)–(A3) leads to the expression

$$\frac{\partial E'}{\partial x'} + \frac{1}{E'}\frac{\partial E'}{\partial t'} + L'\alpha' \exp(-\alpha' x') = 0 . \tag{A6}$$

The nonlinear differential equation has been[16] solved in the coordinate system fixed to the moving charge, and the time dependence of the field has been deduced in the implicit form

$$t'=\frac{\ln\{E'[(1-E')/L']\exp(\alpha' x')+E'\}}{\alpha'[E'-L'\exp(-\alpha' x')]} . \tag{A7}$$

The numerical calculations[16] for $L'\gg 1$ have shown that within the time shorter than the transit time the electric field in the depth $x_0'\approx(\ln L')/\alpha'$ strongly decreases (see Fig. 14).

The decreasing field is related to the screening current within the region $(0-x_0')$ and to the fact that at first only the charge equal to the charge on the electrodes (CU_0), which starts from the position $x_0'=(\ln L')/\alpha'$, can move up to the second electrode (see Fig. 14).

The initial screening current leads to the initial voltage step $\Delta U/U_0\approx(1+\ln L')/\alpha'$ (see Fig. 13). The initial slope of the $U(t)$ transient is proportional to L', which is higher than $\frac{1}{2}$, the typical slope of the theoretical SCLC curve $(\alpha'=\alpha d=\infty)$ (see Fig. 13).

[1]W. E. Spear, in *Advances in Disordered Semiconductors,* Amorphous Silicon and Related Materials Vol. 1, edited by H. Fritzsche (World Scientific, Singapore, 1989), p. 721.

[2]H. Fritzsche, J. Non-Cryst. Solids **114**, 1 (1989).

[3]R. E. Johanson, Y. Kaneko, and H. Fritzsche, Philos. Mag. B **63**, 57 (1991).

[4]G. Juška, G. Jukonis, and J. Kočka, J. Non-Cryst. Solids **114**, 354 (1989).

[5]G. Juška, J. Kočka, K. Arlauskas, and G. Jukonis, Solid State Commun. **75**, 531 (1990).

[6]M. A. Lampert and P. Mark, *Current Injection in Solids* (Academic, New York, 1970), pp. 55 and 119.

[7]J. Kočka, C. E. Nebel, G. H. Bauer, O. Klíma, Y. Xiao, E. Šípek, and G. Juška, *Proceedings of the 20th International Conference on the Physics of Semiconductors* (World Scientific, Singapore, 1990), p. 2059.

[8]J. Kočka, O. Klíma, G. Juška, M. Hoheisel, and R. Plättner, J. Non-Cryst. Solids **137&138**, 427 (1991).

[9]J. M. Marshall, R. A. Street, and M. J. Thompson, Philos. Mag. B **54**, 51 (1986).

[10]G. Seyenhaeve, G. J. Adriaenssens, H. Michiel, and H. Overhof, Philos. Mag. B **58**, 421 (1988).

[11]E. A. Schiff and M. Silver, in *Advances in Disordered Semiconductors,* Amorphous Silicon and Related Materials Vol. 1 (Ref. 1), p. 825.

[12]R. Stachowitz, W. Fuhs, and K. Jahn, Philos. Mag. B **62**, 5 (1990).

[13]C. E. Nebel, J. Non-Cryst. Solids **137&138**, 395 (1991).

[14]M. Kemp and M. Silver, Philos. Mag. B **63**, 437 (1991).

[15]G. Juška, J. Kočka, O. Klíma, and K. Arlauskas, J. Non-Cryst. Solids **137&138**, 411 (1991).

[16]G. Juška, Lith. Phys. J. **30**, 58 (1990).

[17]H. Antoniadis and E. A. Schiff, Phys. Rev. B **43**, 13 957 (1991).

[18]M. Hoheisel, R. Carius, and W. Fuhs, J. Non-Cryst. Solids **63**, 313 (1984).

[19]M. Hoheisel and W. Fuhs, Philos. Mag. B **57**, 411 (1988).